4740 *Biochemistry* **2010,** *49,* 4740–4751
DOI: 10.1021/bi901807p

BIOCHEMISTRY
including biophysical chemistry & molecular biology
Article

Structure and Function of Intact Photosystem 1 Monomers from the Cyanobacterium *Thermosynechococcus elongatus*[†,‡]

Eithar El-Mohsnawy,[§,▽] Marta J. Kopczak,[§] Eberhard Schlodder,[∥] Marc Nowaczyk,[§] Helmut E. Meyer,[⊥] Bettina Warscheid,[@] Navassard V. Karapetyan,[#] and Matthias Rögner*[,§]

[§]*Plant Biochemistry, Ruhr University Bochum, 44780 Bochum, Germany,* [∥]*Max-Volmer Laboratory for Biophysical Chemistry, Technical University, 10623 Berlin, Germany,* [⊥]*Medical Proteom-Center, Ruhr University Bochum, 44780 Bochum, Germany,* [@]*Clinical and Cellular Proteomics, Medical Faculty and Center for Medical Biotechnology, Duisburg-Essen University, 45117 Essen, Germany, and* [#]*A. N. Bakh Institute of Biochemistry RAS, 119071 Moscow, Russia* [▽]*On leave from Department of Biological and Geological Sciences, Faculty of Education in Al-Arish, Suez Canal University, Al-Arish, Egypt.*

Received October 23, 2009; Revised Manuscript Received March 15, 2010

ABSTRACT: Until now, the functional and structural characterization of monomeric photosystem 1 (PS1) complexes from *Thermosynechococcus elongatus* has been hampered by the lack of a fully intact PS1 preparation; for this reason, the three-dimensional crystal structure at 2.5 Å resolution was determined with the trimeric PS1 complex [Jordan, P., et al. (2001) *Nature 411* (6840), 909−917]. Here we show the possibility of isolating from this cyanobacterium the intact monomeric PS1 complex which preserves all subunits and the photochemical activity of the isolated trimeric complex. Moreover, the equilibrium between these complexes in the thylakoid membrane can be shifted by a high-salt treatment in favor of monomeric PS1 which can be quantitatively extracted below the phase transition temperature. Both monomers and trimers exhibit identical posttranslational modifications of their subunits and the same reaction centers but differ in the long-wavelength antenna chlorophylls. Their chlorophyll/P700 ratio (108 for the monomer and 112 for the trimer) is slightly higher than in the crystal structure, confirming mild preparation conditions. Interaction of antenna chlorophylls of the monomers within the trimer leads to a larger amount of long-wavelength chlorophylls, resulting in a higher photochemical activity of the trimers under red or far-red illumination. The dynamic equilibrium between monomers and trimers in the thylakoid membrane may indicate a transient monomer population in the course of biogenesis and could also be the basis for short-term adaptation of the cell to changing environmental conditions.

Photosystem 1 (PS1)[1] is the largest known multisubunit membrane protein complex that functions as a solar energy converter; it catalyzes the transfer of an electron from plastocyanin or cytochrome c_6 on the lumenal side to ferredoxin (or flavodoxin) on the cytoplasmic side. According to X-ray analysis of the trimeric PS1 core complex from the cyanobacterium *Thermosynechococcus elongatus*, the structure exhibits 12 protein subunits and 127 cofactors performing light capturing and electron transfer (*1*−*3*). These cofactors include 96 chlorophylls (Chls), 22 carotenoids (Car), two phylloquinones, three iron−sulfur (4Fe-4S) clusters, and four lipids for each PS1 monomer. The two large subunits, PsaA and PsaB, each consisting of 11 transmembrane helices, coordinate most of the Chls and Cars, and the redox cofactors of electron transport: primary electron donor P700, primary electron acceptor A_0 (Chl *a* monomer), secondary electron acceptor A_1 (phylloquinone), and F_X (iron−sulfur cluster). Terminal electron acceptors F_A and F_B (also iron−sulfur clusters) are both coordinated by the PsaC subunit, which is, with PsaD and PsaE, one of the three extrinsic subunits on the cytoplasmic side. In contrast to eukaryotes, the intrinsic PsaF subunit is not involved in docking of either the electron donor plastocyanin or cytochrome c_6 in cyanobacteria (*4*). Subunits PsaI and PsaL are responsible for formation and stabilization of the PS1 trimer in cyanobacteria (*5*). Subunits PsaK, -M, and -X seem to play a mere structural role.

The PS1 trimer of *T. elongatus* is characterized by a molecular mass of 1068 kDa according to protein and cofactor composition (*1*); i.e., it is the most complex membrane protein for which a molecular structure has been determined. Especially the large content of cofactors provides more than 30% of its total mass. PS1 core complexes from cyanobacteria and higher plants show a high degree of structural similarity (*1*, *6*, *7*), but there are some differences in subunit composition. Subunits PsaX and -M are found only in cyanobacteria and subunits PsaG and -H only in plants. Also, subunit PsaL shows important structural differences

[†]Financial support from the German Research Council, DFG (SFB 480, Project C1, M.R. and M.N.; SFB 498, TP A6, E.S.), the European Union (SOLAR-H project, M.R. and M.J.K.), the Egypt Government (personal grant to E.E.-M.), the Russian Academy of Sciences, program MCB, and RFBR (Grant 08-04-00143a, to N.V.K.) is gratefully acknowledged.

[‡]Dedicated to Prof. Dr. Achim Trebst on the occasion of his 80th birthday.

*To whom correspondence should be addressed: Ruhr-Universität Bochum, Universitätsstr. 150, 44780 Bochum, Germany. Telephone: +49 (234) 322-3634. Fax: +49 (234) 321-4322. E-mail: Matthias.Roegner@rub.de.

[1]Abbreviations: Car, carotenoid; Chl, chlorophyll; DPIP, 2,6-dichlorophenolindophenol; Lhca1−Lhca4, light-harvesting complexes of plant PS1; LWC, long-wavelength chlorophylls; MV, methyl viologen; PS1 and PS2, photosystem 1 and photosystem 2, respectively; P700 and $P700^+$, primary electron donor of PS1 in the reduced and oxidized state, respectively; β-DM, *n*-dodecyl β-D-maltoside; PsaA, PsaB, etc., polypeptide subunits of the PS1 complex; RT, room temperature; +ST and −ST, salt-treated and non-salt-treated membranes, respectively.

 Published on Web 04/01/2010

which may be the reason for a different supramolecular organization (*5*). Cyanobacterial PS1 was reported to exist preferably as a trimeric complex (*3*, *8*−*11*), whereas plant PS1 apparently is exclusively monomeric, most probably due to binding of peripheral Lhca1−Lhca4 complexes (*12*−*14*) and/or PsaH preventing trimerization (*3*, *13*, *15*, *16*).

A high content of the so-called long-wavelength Chls (LWC; also red or low-energy Chls) absorbing at energies lower than that of P700 is a unique property of many cyanobacterial PS1 core antennae (*9*, *17*−*21*). The content and the spectral characteristics of LWC are highly species-dependent (*20*, *22*), with PS1 trimers containing usually more red Chls than PS1 monomers (*23*). Five kelvin absorption spectra of PS1 trimers from *T. elongatus* exhibit Chl *a* antenna states absorbing at 708 and 719 nm (*24*−*27*), whereas PS1 trimers of *Synechocystis* sp. PCC 6803 (hereafter called *Synechocystis*) contain LWC peaking at shorter wavelengths, 708 and 714 nm (*28*, *29*). The most red-shifted Chl antenna state absorbing at 708 and 740 nm and emitting at 760 nm (77 K) was observed in PS1 trimers of *Arthrospira* (*Spirulina*) *platensis* (*9*, *30*, *31*). The fluorescence of LWC in these PS1 trimers of *A. platensis* is quenched by oxidized P700 or P700 in the triplet state (*9*, *30*, *32*). The dependence of the fluorescence yield of the red-most Chl in PS1 trimers of *A. platensis* and *T. elongatus* on the redox state of P700 allowed to follow the processes of energy utilization and dissipation in PS1 (*26*, *30*, *33*). Overall, the presence of LWC in many types of PS1 complexes of cyanobacteria indicates their functional importance. Energy absorbed by these LWCs migrates uphill to P700 and causes its oxidation (*34*, *35*). As the same 77 K fluorescence band at 760 nm was found in isolated PS1 trimers, in membranes, and in whole cells of *A. platensis*, this was the direct evidence for preexisting PS1 trimers in membranes of cyanobacteria (*9*, *31*). Moreover, differences in the fluorescence emission spectra of PS1 trimers and monomers of *A. platensis* at 77 K helped to indicate a dynamic equilibrium of the monomer/trimer ratio within the detergent-free membranes and an energy exchange between PS1 monomers within a trimer (*30*, *36*).

Trimeric PS1 from the cyanobacterium *T. elongatus* is the most stable PS1 from which also the most resolved three-dimensional (3D) structure has been determined (*1*). To understand the functional interaction of the three monomers within this well-characterized trimer, which is in turn the prerequisite for forming a conclusion about its physiological significance, a quantitative preparation procedure for "nativelike" PS1 monomers is required. This is hampered by the fact that a routine extraction from the thylakoid membrane of *T. elongatus* yields nearly exclusively trimeric complexes. In the past, attempts to isolate monomeric PS1 from *T. elongatus* involved special detergent treatment using Triton X-100 (*37*), β-octyl glucopyranoside at elevated temperatures (*38*), or sodium dodecyl sulfate and sodium cholate (*8*, *39*), pre-extraction of carotenoids using *n*-heptane (*40*), or deletion of the central PsaL subunit (*3*, *11*, *41*−*43*), which apparently is required for trimerization (*44*). All these attempts resulted in structural and/or functional defects. Using the detergent *n*-dodecyl β-D-maltoside (β-DM) in combination with an osmotic treatment during the passage through a gel filtration column, Jekow et al. succeeded in partially dissociating PS1 trimers into monomers (*45*). However, depending on the detergent (β-DM or sulfobetaine), these monomers showed a distinctly reduced Chl antenna size and the loss of PsaL and -K subunits in comparison with PS1 trimers. In any case, the activity of the obtained monomeric complexes was considerably reduced, leading to the assumption that only trimeric PS1 represents the fully active PS1 form. This was supported by the impaired growth under low-light conditions of *T. elongatus* cells which contained only monomeric PS1 due to *psaL* deletion (*11*, *46*). In contrast, 3D crystals of *T. elongatus* PS1 reveal 96 Chls (*1*), and the antenna size of PS1 within cells of the cyanobacterium *A. platensis* was even calculated to be 120 Chls (*47*), indicating that all published methods resulting in monomeric-like PS1 do not reflect the structure and organization of PS1 in the cell and are not suited for comparison with their trimeric counterparts.

To combine high-resolution structural data with detailed functional characterization of PS1 and also to learn about the smallest functional PS1 unit, we made an attempt to isolate monomeric PS1 from *T. elongatus*. Preservation of subunit composition was achieved by dissociation of trimers into monomers within the membrane phase using high salt prior to extraction as reported previously for a mesophilic organism (*48*). The intactness of this preparation, which was also confirmed by comparison with a salt-free isolated preparation using an extremely low detergent concentration for extraction, enabled for the first time the in depth characterization of a nativelike monomeric PS1 in comparison with its trimeric counterpart using both structural and functional state-of-the-art analytical methods. In addition, this comparison yields information about functional interactions of the monomers within the trimer, including the special role of the long-wavelength Chls.

EXPERIMENTAL PROCEDURES

Cell Culture and Preparation of the PS1 Extract. *T. elongatus* cells were grown in BG11 medium (*49*), harvested, and disrupted using a Parr bomb at 4 °C according to established protocols (*38*, *50*, *51*). Fresh thylakoid membranes {in buffer A [0.5 M mannitol, 20 mM HEPES (pH 7.5), 10 mM $MgCl_2$, and 10 mM $CaCl_2$]} or frozen thylakoid membranes [in buffer D (buffer A with 20% glycerol)] were adjusted to a Chl concentration of approximately 0.75 mg/mL (in ∼100 mL) with buffer A, homogenized five times, and centrifuged for 20 min at 8100*g* (JLA-16.250 rotor, Beckman). In the case of isolation of PS1 monomers and trimers [with salt treatment (Chart 1)], the pelleted thylakoid membranes have been washed three times with buffer A containing 0.05% β-DM to remove the phycobilisomes. The pellet of the phycobilisome-depleted thylakoid membranes was resuspended and incubated for 20 min in high-salt extraction buffer (temperature as indicated) at 1 mg/mL Chl, followed by extraction with β-DM (0.6%) and ultracentrifugation (1 h at 180000*g*). For the isolation of PS1 monomers from non-salt-treated (−ST) membranes, they were suspended in 0.1% β-DM and centrifuged at 8100*g* for 20 min. After the salt concentration had been adjusted to 1 M $(NH_4)_2SO_4$ [using buffer A containing 2 M $(NH_4)_2SO_4$], most of the phycobilisomes were pelleted by ultracentrifugation (1 h at 180000*g*).

Chromatographic Purification and Analysis of PS1. With the exception of analytical SEC (see below), all chromatographic purification was performed on a PerSeptive Biocad 700 E chromatography system (Applied Biosystems). A POROS 50 OH HIC column (Applied Biosystems) was used as the first purification step for PS1 monomers and trimers. After column equilibration [buffer consisting of 20 mM HEPES (pH 7.5), 1.5 M ammonium sulfate, 10 mM $MgCl_2$, 10 mM $CaCl_2$, 0.5 M mannitol, and 0.03% β-DM)], extracted PS1 complexes were

Chart 1: Preparation Steps for the Isolation and Purification of Monomeric and Trimeric PS1 Involving a Salt Treatment Step (+ST)

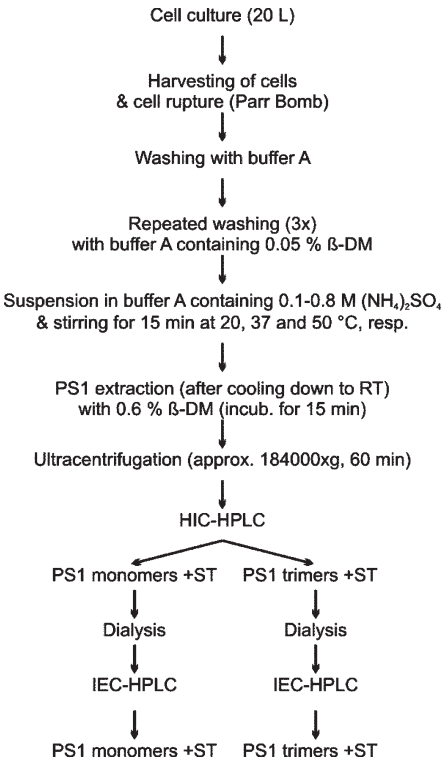

mixed with ammonium sulfate for a final concentration of 1.5 M (150 mS) and loaded onto the column. PS1 was eluted by a linear gradient (1.5 to 0 M) or by two gradient steps (from 1.5 to 1.1 M and from 1.1 to 0 M, in the case of PS1 from non-salt-treated membranes) of ammonium sulfate at a flow rate of 5 mL/min. Purified PS1 was dialyzed against buffer [20 mM HEPES (pH 7.5), 10 mM $MgCl_2$, 10 mM $CaCl_2$, 0.5 M mannitol, and 0.03% β-DM] overnight at 10 °C before IEC was started as a second purification step. The POROS HQ/M (Applied Biosystems) IEC column was used as a second purification step. After column equilibration [buffer consisting of 20 mM HEPES (pH 7.5), 10 mM $MgCl_2$, 10 mM $CaCl_2$, 0.5 M mannitol, and 0.03% β-DM], dialyzed PS1 was loaded onto the column and eluted by a linear gradient (0 to 200 mM) of $MgSO_4$.

MALDI-TOF Analysis of Intact Protein Complexes. Intact PS1 subunits were analyzed by MALDI-TOF mass spectrometry according to the method described in ref *52*. PS1 in buffer [20 mM HEPES (pH 7.5), 10 mM $MgCl_2$, 10 mM $CaCl_2$, and 0.03% β-DM] at a Chl concentration of 0.2−0.3 μg/μL was mixed in a 1/1 ratio with a saturated matrix solution [sinapic acid or ferulic acid in 1% trifluoroacetic acid and 60% (v/v) acetonitrile], spread on the target plate (0.6 μL), and air-dried before being used. Analysis was performed on a MALDI-TOF mass spectrometer (Voyager DE, Applied Biosystems) or alternatively on a qTOF mass spectrometer (QSTAR XL, Applied Biosystems). Calibration was conducted with standard proteins (Mix 3, Sequazyme Kit, Applied Biosystems).

Determination of Chl a, Car, and P700 Concentrations. Chlorophyll concentrations were measured in an 80% (v/v) acetone/water mixture and calculated according to the method described in ref *53*. The Chl/P700 ratio for the PS1 complexes was calculated from the maximal flash-induced absorption change in the Q_Y region due to the photooxidation of P700, using a differential molar extinction coefficient ($\Delta\varepsilon$) of 61000 ± 2000 M^{-1} cm^{-1} (*54*).

The Car content was determined from the absorption spectrum of the pigment extract in an 80% acetone/water mixture according to the method described in ref *55*, using a Cary-1E-UV/vis spectrophotometer. The absorption spectrum of Car was obtained by subtraction of the spectrum of pure Chl *a* in an 80% acetone/water mixture that has been normalized to the absorption of the extract in the Q_Y region. The Chl *a*/Car ratio was calculated according to the following equation:

$$\frac{\text{Chl } a}{\text{Car}} = \frac{A_{664}/\varepsilon_{664}}{A_{450}/\varepsilon_{450}}$$

The following extinction coefficients were used: 76800 M^{-1} cm^{-1} at 664 nm for Chl *a* (*53*, *56*) and 134000 M^{-1} cm^{-1} at 450 nm for β-carotene (*57*).

Absorption Spectra. Low-temperature (5 K) absorption spectra were recorded at a resolution of 0.5 or 1 nm in a Cary-1E-UV/vis spectrophotometer equipped with an Oxford liquid helium flow cryostat (CF1204, Oxford). The purified PS1 sample was diluted to an OD_{680} of ~1 in buffer [20 mM MES, 20 mM $CaCl_2$, 10 mM $MgCl_2$, 5 mM sodium ascorbate, 0.02% β-DM, and 60−65% glycerol (pH 6.5)].

To analyze the number of Chls contributing to the red absorption, we decomposed the red region (685−750 nm) of the 5 K absorbance spectra into Gaussian bands (*32*). We obtained the number of Chls contributing to the red absorption from the ratio of the integrated intensity of the long-wavelength absorption bands at 710 and 720 nm to the total integrated intensity of the Q_Y band and the number of Chls per PS1.

Fluorescence Spectra. Fluorescence emission spectra (600−800 nm, excitation at 440 nm) were recorded in a SLM-AMINCO Bowman, Series 2 luminescence spectrometer at RT or 77 K. The Chl concentration of the PS1 samples was adjusted with buffer [20 mM HEPES (pH 7.5), 10 mM $MgCl_2$, 10 mM $CaCl_2$, 0.02% β-DM, and 60% glycerol] to 5−8 μg/mL for measurements at RT and to 3 μg/mL for 77 K.

PS1-Mediated Electron Transport Rates. The photochemical activity of PS1 was determined by measuring the oxygen uptake according to the Mehler reaction induced by actinic light in a fiber optic oxygenmeter (FIBOX 2, PreSens). For activity measurements, the concentrated purified PS1 complexes were diluted with PS1 activity buffer [30 mM HEPES (pH 7.5), 3 mM $MgCl_2$, 50 mM KCl, 330 mM mannitol, and 0.03% β-DM] to a final Chl concentration of 3−5 μg/mL. 2,6-Dichlorophenolindophenol (800 μM) and sodium ascorbate (5 mM) were used as electron donors, and methyl viologen (0.5 mM) was used as an electron acceptor. The sample was stirred in darkness for 2 min. Three actinic lights have been used: white light (20000 μE m^{-2} s^{-1}), red light (λ > 665 nm, 4000 μE m^{-2} s^{-1}), and far-red light (λ > 715 nm, 700 μE m^{-2} s^{-1}). As a source of actinic light, a KL2500 LCD (Schott) was used. Calibration of the sensor and all measurements was conducted at 30 °C.

Transient Absorption Spectroscopy. Flash-induced absorbance changes were measured with the setups described previously (*54*). Flash-induced absorbance difference spectra of $P700^+$ minus P700 at RT were measured with PS1 complexes diluted to 10−15 μg/mL Chl in 20 mM Tricine (pH 7.5), 25 mM $MgCl_2$, 100 mM KCl, 0.02% β-DM, 5 mM sodium ascorbate, and 10 μM PMS. $P700^+F_{A/B}^-$ minus $P700F_{A/B}$ spectra recorded at 5 K were obtained by subtracting the absorption spectra of PS1

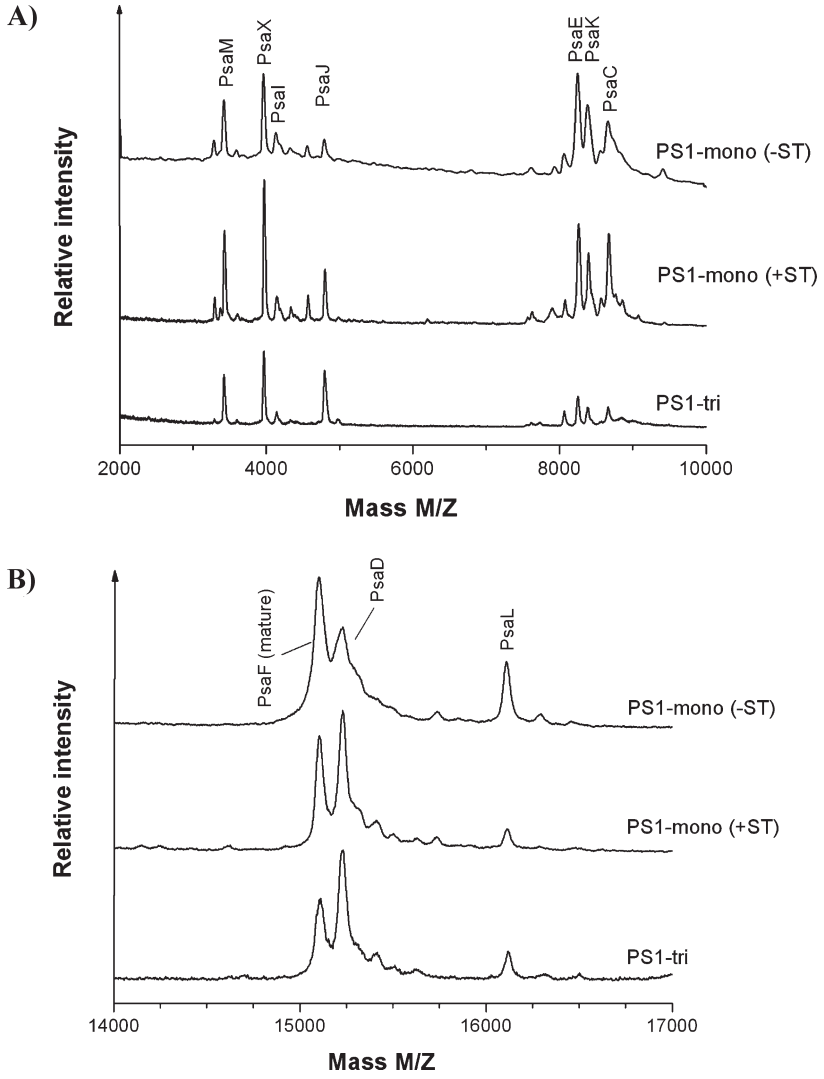

FIGURE 1: MALDI-TOF MS analysis of purified PS1 monomers and trimers from *T. elongatus*. Purified PS1 complexes were mixed in a 1/1 ratio with ferulic acid, and 0.6 μL of this mixture was air-dried on the target plate before being analyzed in the mass spectrometer (Voyager DE MALDI-TOF). Covered mass range: 2000−10000 (A) and 14000−17000 (B).

in the dark-adapted state with P700 reduced from those measured after illumination. The concentration of the PS1 complexes and the buffer composition were identical to those at RT, but the buffer contained 60−65% glycerol.

RESULTS

Development of a Preparation Procedure for Nativelike Monomeric PS1. Chart 1 summarizes the developed strategy for the enrichment of monomeric PS1 in the thylakoid membrane prior to extraction, isolation, and purification. This method is mainly based on the dissociation of trimeric PS1 complexes within the membrane by a special salt treatment which has been shown previously for PS1 from the mesophilic cyanobacteria *Synechocystis* (*48*) and *A. platensis* (*30*). Prerequisite for an efficient salt treatment is the minimization of PBS content by a low-concentration β-DM wash (0.05%). For the subsequent process of salt dissociation, several salts have been tested: NaCl, $CaCl_2$, $MgCl_2$, $MgSO_4$, and $(NH_4)_2SO_4$. While NaCl, $CaCl_2$, and $MgCl_2$ exhibited a very low efficiency in dissociating trimers into monomers as judged from elution profiles of HIC columns or sucrose density gradients (for details, see the Supporting Information), $MgSO_4$ was partially effective and ammonium sulfate was the most efficient. If this salt treatment was combined with an incubation at 50 °C, followed by an extraction at RT, the highest monomer/trimer ratio could be gained. Saturation of this effect was observed at 0.6 M ammonium sulfate at 50 °C. Distinctly lower ratios obtained with salt incubation at 20 or 37 °C indicate that the liquid-crystalline state [>37 °C (M. Hato, personal communication)] is the prerequisite for the extraction of PS1 monomers in substantial amounts.

After extraction, PS1 monomers and trimers can be gained at high purity and homogeneity by two-dimensional chromatography, consisting of an HIC-HPLC column step, followed by IEC-HPLC. These fractions were then used for a detailed biochemical and biophysical characterization.

MALDI-TOF Analysis of Monomeric versus Trimeric PS1: What Is the Smallest Fully Functional Unit? Potential structural differences between monomers and trimers have been investigated by a detailed MALDI-TOF analysis (Figure 1). To exclude the secondary effects of the salt treatment on the monomers, for comparison monomers that have not been exposed to any salt have also been used (−ST). Additionally, the detergent concentration used for extraction (0.1% instead of 0.6% β-DM) and the exposure time (5 min instead of 15 min at RT) was minimized to help keep the monomer in its nativelike

Table 1: PS1 Subunit Modifications of Monomeric and Trimeric PS1 According to MALDI-TOF MS Analysis (see Figure 1)

subunit	determined mass[a] (Da)	calculated mass[a] (Da)	difference (Da)	modification	mass spectrometer (matrix)
PsaA	not detected	83183	–	–	–
PsaB	not detected	82913	–	–	–
PsaC	8669.1	8800.1	−131	*N*-methinone deleted	qTOF QSTAR XL (Sinapic)
PsaD	15240.8	15370.5	−129.7	*N*-methinone deleted	qTOF QSTAR XL (Sinapic)
PsaE	8259.1	8388.5	−129.4	*N*-methinone deleted	qTOF QSTAR XL (Sinapic)
PsaF (mature)	15114.3	15113.4	+0.9	cleaved N-terminus	qTOF QSTAR XL (Sinapic)
PsaI	4195.6	4166	+29.6	formyl group added	qTOF QSTAR XL (Sinapic)
PsaJ	4796.1	4766.7	+29.4	formyl group added	qTOF QSTAR XL (Sinapic)
PsaK	8390.1	8480	−89.9	*N*-methinone deleted and acetyl group added	qTOF QSTAR XL (Sinapic)
PsaL	16118	16251	−133	*N*-methinone deleted	Voyager DE (Ferulic)
PsaM	3424.4	3424.1	+0.3	no modification	qTOF QSTAR XL (Sinapic)
PsaX	3969.8	4100.9	−131.1	*N*-methinone deleted	qTOF QSTAR XL (Sinapic)

[a]Mass spectrometers: qTOF QSTAR XL and Voyager DE (for details, see Experimental Procedures). Theoretical calculations of PS1 subunits are based on data from CyanoBase.

structure, even at the expense of a nonquantitative extraction (the amount of extracted monomer is around 1% of the standard procedure).

The determined masses of this analysis, which are summarized in Table 1, show the presence of all PS1 subunits known from the 3D crystal structure analysis (*1*); however, subunits PsaA and PsaB could be identified only by SDS−PAGE because of their high mass (not shown). Most remarkably, subunit PsaL which is easily lost upon dissociation of trimeric PS1 (*44*, *45*) is present in both monomeric PS1 fractions, which was also confirmed by immunoblotting (not shown). This indicates the mild conditions of both purification procedures, with the untreated PS1 monomer showing a slightly higher PsaL content in the immunoblot than the salt-treated complex (+ST).

For the first time, this analysis also shows that all PS1 subunits below 20000 Da with the exception of PsaM are post-translationally modified (see Table 1). The N-terminal methionine was removed from six subunits (PsaC, PsaD, PsaE, PsaK, PsaL, and PsaX), whereas it remained formylated in two subunits (PsaI and PsaJ). PsaK was shown to be additionally acetylated, and N-terminal processing was confirmed for the PsaF subunit (*58*).

For the evaluation of the quantitative PS1 monomer preparation involving salt treatment, it is important that no mass deviation due to high temperature or high salt concentration was observed.

Spectroscopic Analysis of Monomeric versus Trimeric PS1. Spectral differences that most likely result from subtle structural differences between PS1 monomers and trimers can be revealed by comparing absorption spectra and absorption difference spectra of the purified complexes. Figure 2 shows that 5 K absorption spectra of PS1 monomers resemble closely those of trimers except that trimers exhibit higher absorption in the far-red region (710−725 nm). The fact that both types of monomers exhibit identical spectra indicates that the combination of high temperature with high salt treatment during the isolation of the monomeric complexes did not affect their spectral properties. The small shoulder at 683.5 nm observed in both PS1 monomers might indicate a rearrangement of some Chl molecules during trimerization, resulting in more far-red Chls in the trimer at 720−725 nm at the expense of the Chl absorption between 680 and 85 nm. To obtain more quantitative information about the red-most chlorophylls, we decomposed the 5 K absorption spectra of PS1 monomers and trimers in the red region by seven Gaussian bands. The number of chlorophylls contributing to the

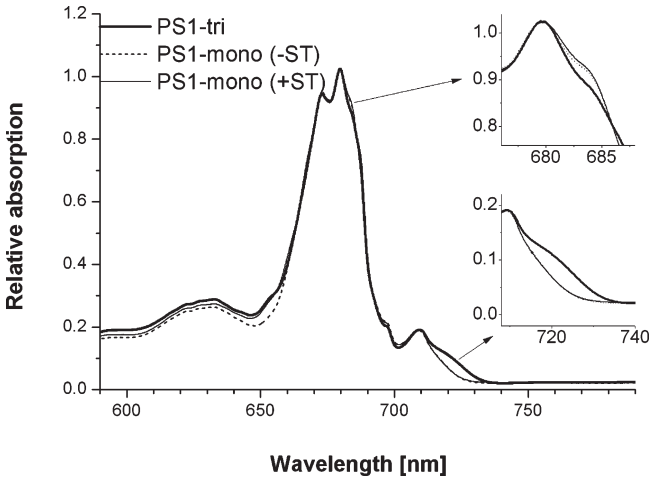

FIGURE 2: Absorption spectra (5 K) of PS1 monomers and trimers (buffer consisting of 20 mM HEPES, 10 mM $CaCl_2$, 10 mM $MgCl_2$, 60% glycerol, and 0.03% β-DM).

red absorption can be estimated from the integrated intensity of the long-wavelength absorption band to the total intensity of the Q_Y band and the number of chlorophylls per PS1. Both PS1 monomers are characterized by two LWCs absorbing at 720 nm and five or six LWCs absorbing at 710 nm (Table 2). In contrast, PS1 trimers exhibit approximately four LWCs absorbing at 720 nm, while there are also five LWCs at 710 nm, in agreement with data obtained previously for PS1 trimers of *T. elongatus* (*2*, *24*).

Figure 3A shows that flash-induced absorption difference spectra of PS1 monomers and trimers attributed to the formation of $P700^+F_{A/B}^-$ are virtually identical at RT. Figure 3B presents the $P700^+F_{A/B}^-$ minus $P700F_{A/B}$ spectra measured at 5 K. These spectra were obtained by subtraction of the absorption spectra of PS1 in the dark-adapted state, with P700 reduced from those measured after illumination. These difference spectra exhibit a broad bleaching around 703 nm, a strong absorbance increase at 691 nm, a further bleaching at 685 nm, and several additional narrow bands because of the higher spectral resolution at 5 K (see ref *25* for a discussion). Figure 3B reveals also that the high-resolution spectra detected at 5 K with PS1 monomers and trimers are almost identical, indicating the spectral properties and the arrangement of the reaction center pigments are the same in the isolated complexes. In addition, P700 of PS1 monomers and trimers is characterized by the same midpoint potential (Table 2).

Table 2: Chl *a*/P700 Ratio, Carotenoid Content, Long-Wavelength Chlorophylls (LWCs), Photochemical Activity, and P700 Midpoint Redox Potential of Purified Monomeric and Trimeric PS1 Complexes

	trimers	monomers
Chl *a*/P700	112 ± 7	108 ± 7
carotenoid content per monomer	22 ± 1	22 ± 1
LWC content[a] (710 nm/720 nm)	5/4	5−6/2
oxygen uptake (WL[c])	1330 ± 50	1330 ± 50
oxygen uptake[b] (RL[d])	1100	850
oxygen uptake[b] (FR[e])	720	520
midpoint potential of P700[a] (mV)	443	442

[a]The LWC (with absorption peaks at 710 and 720 nm) contents were determined from 5 K absorption spectra of the corresponding PS1 complexes by Gaussian deconvolution; the photochemical activity is determined as light-induced oxygen uptake (see Experimental Procedures), and the P700 midpoint potential is determined by titration of light-induced absorption changes at 700 nm. [b]Photochemical activity in micromoles of O_2 per milligram of Chl per hour. [c]WL, white light. [d]RL, red light. [e]FR, far-red light.

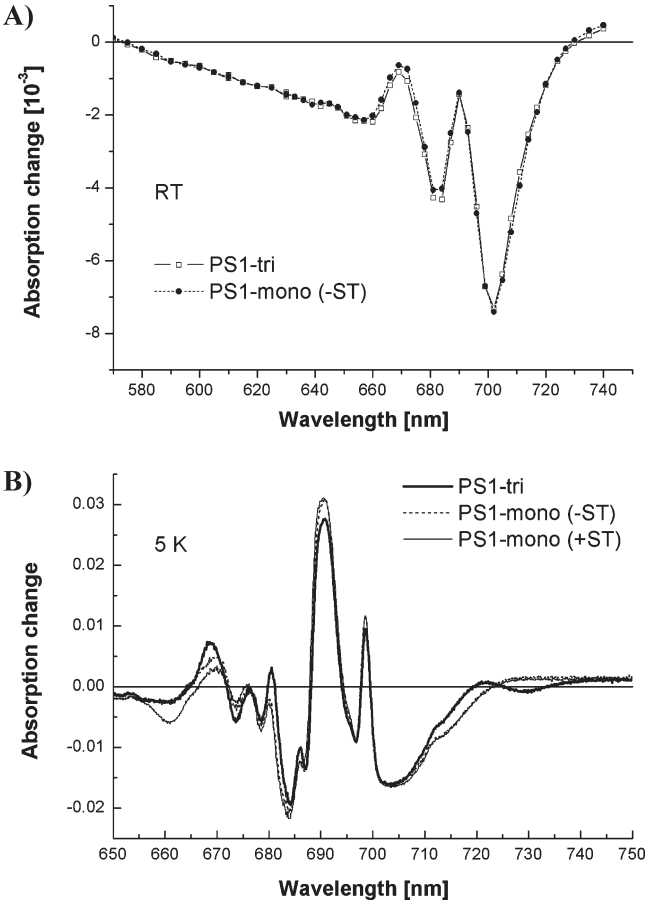

FIGURE 3: Flash-induced $P700^+$ minus P700 absorbance difference spectra of trimeric and monomeric PS1 complexes at RT (A) and $P700^+F_{A/B}^-$ minus $P700F_{A/B}$ spectra measured at 5 K. These spectra were recorded by subtraction of the absorption spectra of PS1 in the dark-adapted state, with P700 reduced from those measured after illumination at 5 K (B).

Different approaches have been used to analyze the pigment composition of PS1 monomers and trimers. To determine the number of Chls per PS1, we measured the concentration of Chl and the content of P700 for the different samples. The P700 concentration was calculated from the maximal absorption decrease in the Q_Y region at ~702 nm using an extinction difference coefficient $\Delta\varepsilon$ of 61000 ± 2000 M^{-1} cm^{-1}. The identical absorption difference spectra of monomeric and trimeric PS1 complexes (see Figure 3) show that the same $\Delta\varepsilon$ value might be used. Using these $\Delta\varepsilon$ values, we obtained the following ratios: 112 for PS1 trimers, 108 for native PS1 monomers, and 109 for salt-treated PS1 monomers (Table 2). The average Chl/P700 ratio for the trimer is slightly higher than for the monomers, but distinctly higher than the level of 96 Chls per monomer as determined from the X-ray structure (*1*). We can, however, not exclude that the reason for this discrepancy is the difference in the extinction coefficient taken from the literature (*54*). Using redissolved crystals of PS1 trimers from *T. elongatus* yielded ~102 ± 6 Chls per P700 with a $\Delta\varepsilon$ of 61000 M^{-1} cm^{-1} (*55*), whereas only 96 Chls have been identified in the 2.5 Å structure (*1*). This could indicate that the $\Delta\varepsilon$ value might be slightly higher.

The Car content was determined by analyzing the spectrum of the pigment extract in an 80% acetone/water mixture (see Experimental Procedures). Both PS1 monomers and trimers yielded the same ratio of Chl *a* to Car of 4.55 ± 0.05 (not shown). On the basis of this value and assuming ~100 Chls per PS1, 22 ± 1 Car have been calculated per PS1 monomer and trimer (Table 2), which is identical to the Car content determined from the 3D structure, i.e., 22 Cars.

The most remarkable difference between purified PS1 monomers and trimers of *T. elongatus* was revealed in 77 K fluorescence emission spectra (Figure 4A). PS1 monomers peaked at 727 nm, while trimers peaked at 732 nm. This characteristic red shift of 5 nm confirms the higher LWC content of the trimers. Furthermore, the symmetric form of the observed spectra in Figure 4A is a good indication of the purity of the isolated PS1 complexes.

Fluorescence emission spectra of the various PS1 preparations at RT show a shoulder at 688−695 nm in both monomers, which is significantly smaller in trimers (Figure 4B). It is also observed that the shoulder at 695 nm in untreated monomers (−ST) shifts to 688 nm with salt treatment (+ST). Most probably, this is an effect of the bound detergent concentration, which is higher for the detergent-exposed monomers than for trimers, and also higher for salt-treated monomers than for "native" monomers. Remarkably, the presented data show only very small (or no) fluorescence at 680 nm, which is typical for uncoupled Chls; this confirms the high quality of the PS1 preparations.

To determine the functional activity of the purified PS1 monomers and trimers, we measured the rate of transfer of an electron from DPIP and ascorbate to methyl viologen as oxygen uptake (Mehler reaction) under continuous illumination at 30 °C (Table 2). White light illumination of isolated PS1 monomers and trimers showed (within the range of error) very similar oxygen uptake activity at a very high level, i.e., 1330 ± 50 μmol of O_2 (mg of Chl)$^{-1}$ h^{-1}. Illumination with red light (λ > 665 nm) resulted in a decrease in activity that was larger in the case of PS1 monomers than of PS1 trimers [850 and 1100 μmol of O_2 (mg of Chl)$^{-1}$ h^{-1}, respectively]. An even greater decrease was found for the illumination with far-red light (λ > 715 nm): 520 and 720 μmol of O_2 (mg of Chl)$^{-1}$ h^{-1}, respectively.

DISCUSSION

Reasoning behind the Preparation of Nativelike PS1 Monomers. While the structure of the monomeric complex can be deduced from the 3D crystal structure of the trimer

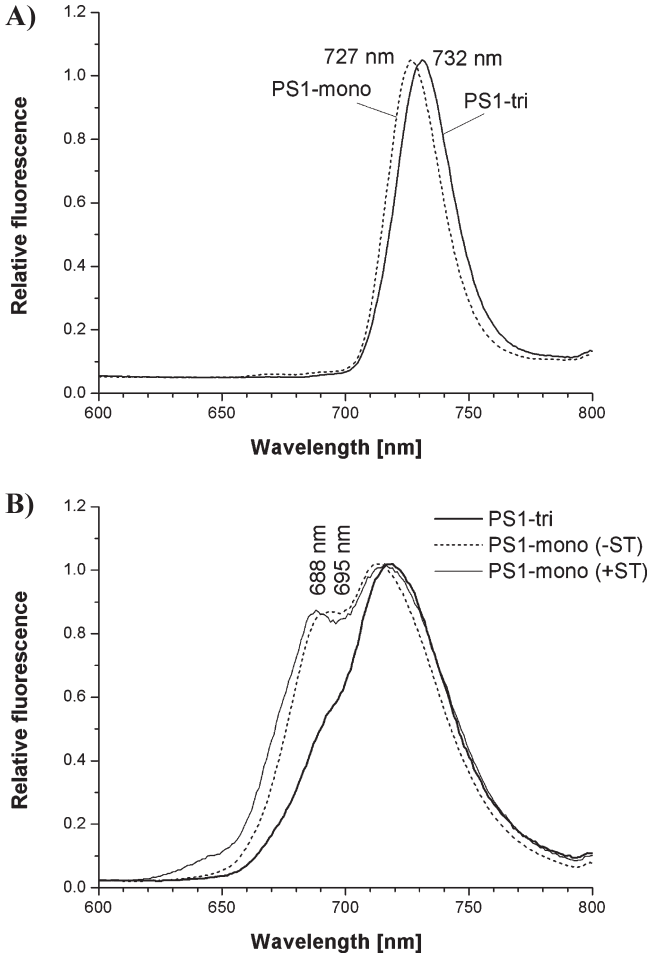

FIGURE 4: Fluorescence emission spectra of different PS1 preparations. (A) The 77 K fluorescence spectra of PS1 monomers and trimers; excitation at 440 nm [buffer consisting of 20 mM HEPES (pH 7.5), 10 mM $CaCl_2$, 10 mM $MgCl_2$, 0.5 M mannitol, 0.03% β-DM, and 60% glycerol]. (B) Fluorescence emission spectra of PS1 monomers and trimers at RT; conditions as for panel A, but without glycerol. The spectra were normalized by maximum intensity.

isolated from *T. elongatus* (*1*), the functional implications of three monomers being merged into one trimer in comparison with the function of the individual PS1 monomer can only be determined if a close-to-native preparation of the monomeric complex is available. Until now, various attempts have been made to isolate nativelike PS1 monomers from *T. elongatus*. Among them was the deletion of the trimer-stabilizing PsaL subunit (*3*, *11*, *41*, *42*), an osmotic pressure treatment (*45*), the extraction by β-octyl glucopyranoside at elevated temperatures (*38*), and the use of mutants with impaired phosphatidylglycerol synthesis which apparently is required for trimerization (*44*). All these attempts resulted in partly damaged monomeric PS1 complexes that lacked one or more subunits, especially PsaL and/or pigment molecules (Chl and Car) to various degrees (*45*). In any case, the activity of these complexes was considerably reduced, leading to the assumption that only trimeric PS1 represents the fully active PS1 form. This was supported by the fact that *T. elongatus* cells with deleted *psaL*, which contained only monomeric PS1, exhibited impaired growth under low-light conditions (*11*, *46*).

In the special case of *T. elongatus,* major reasons for the previous failing to isolate nativelike (i.e., with structural and functional integrity) PS1 monomers might be their small amount in the cells under the preparation conditions (*46*), their (partial) loss during washing with 0.1% β-DM (*44*), and/or the overlay of PS1 monomers with the PS2 band in the sucrose density gradient (*50*). Results of this study suggest that PS1 complexes preexist in both monomeric and trimeric form within the thylakoid membrane of *T. elongatus*, and that it is possible, if care is taken, to isolate PS1 monomers in their native form for further characterization.

Prerequisite for a detailed characterization of monomeric PS1 complexes is the possibility to isolate them in larger quantities from the cells. As several reports have already shown, it is apparently impossible to gain nativelike monomers from isolated trimers, which are dissociated, for instance, by detergent treatment (*50*). The only promising strategy is to dissociate trimers within the thylakoid membrane into monomers before extracting them with detergent. In principle, this is possible by a high-salt treatment of the membranes as shown previously for mesophilic cyanobacterial cells (*59*) and confirmed in this report for *T. elongatus*. However, in contrast to the mesophile, the optimal salt concentration was considerably higher for the thermophile (500−600 mM vs 150−200 mM), and the type of salt (i.e., divalent or monovalent ions) had a severe impact on its effect. Apparently, divalent sulfate anions are most effective in screening electrostatic surface charges, suggesting cationic counterions on the PS1 surface are affected by it.

This organism provides an additional unique property. Because of its thermophilicity, the phase transition temperature of its membranes is considerably higher than in mesophilic organisms such as *Synechocystis* (*60*) which can be used to immobilize or "freeze" transient compositions of the membranes. At temperatures below the phase transition point, complexes can be extracted from the membrane in their existing oligomeric status without sufferng a major impact of the detergent. Most probably, this is due to the fact that the detergent replaces the lipids that surround these complexes in their native state.

In the case of PS1, this situation is illustrated by the model shown in Figure 5. Upon high-salt incubation above the phase transition temperature, many PS1 trimers dissociate into monomers (Figure 5A,B). Apparently, the added ammonium sulfate ions neutralize charges in the monomer−monomer interface, in which calcium ions may also be involved because of their impact on trimerization (*46*). This may help to weaken electrostatic forces (*61*) and enable lipids to diffuse into the interface (which is also promoted by the elevated temperature). These lipids help to weaken the hydrophobic interaction between the monomers, since their hydrophobic tails can act as a kind of shield for the membrane-embedded parts of the proteins (*48*). The status of salt-induced monomerization is conserved by rapidly lowering the temperature to 20 °C, i.e., distinctly below the phase transition temperature (Figure 5C). At 20 °C, both monomeric and trimeric complexes can be extracted by a mild detergent treatment, during which the detergent β-DM partly replaces the lipids that shield the protein during extraction. As neither a dissociation of isolated trimers into monomers nor an association of isolated monomers into trimers is possible under our experimental conditions (*61*), the ratio of extracted monomers to trimers (as evidenced after chromatographic separation) most probably reflects the ratio present in the membrane in response to the ammonium sulfate concentration and the chosen temperature (Figure 5D). If these conditions are chosen appropriately, PS1 monomers can be extracted in quite large amounts which is the prerequisite for their in depth characterization in comparison with the trimers.

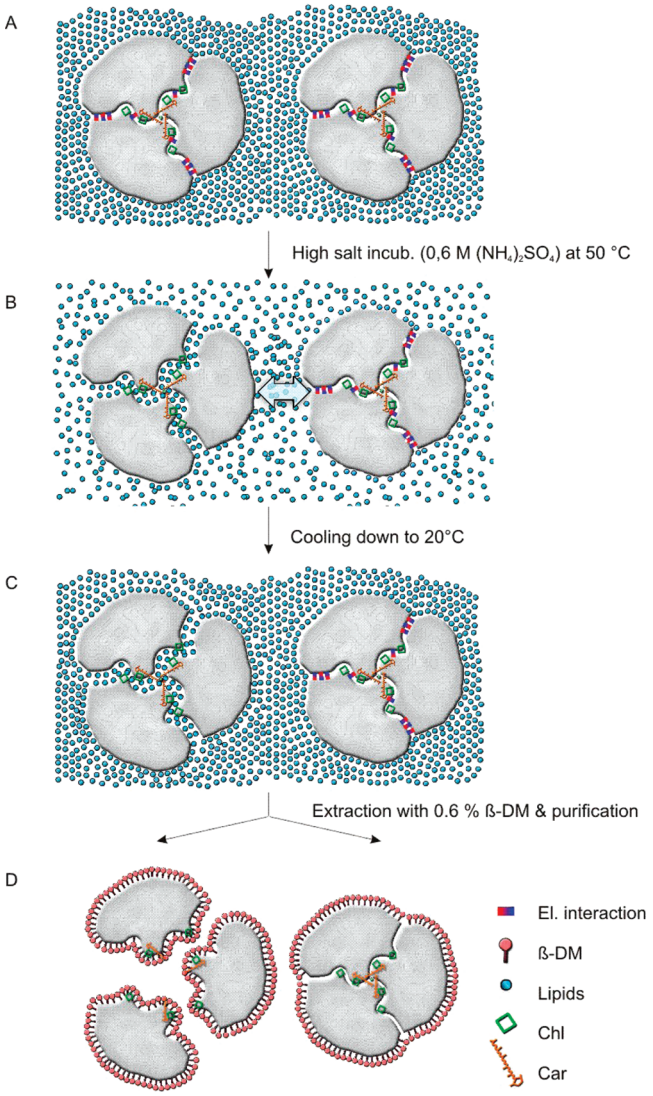

FIGURE 5: Model illustrating the experimental steps taken to monitor the equilibrium between PS1 monomers and trimers in the thylakoid membrane of *T. elongatus*. (A) At <30 °C (solid lipid phase), PS1 trimers are surrounded by lipids. Hydrophobic interaction (i.e., the central PsaL subunit in combination with Chl and Car) and electrostatic interaction (involving Ca^{2+} ions) may help to stabilize the trimer. (B) Heating to 50 °C (mobile lipid phase) in the presence of a high salt concentration. Weakened electrostatic interactions between PS1 monomers due to increased ion concentration. Diffusion of lipids into the PS1 trimer contact area weakens hydrophobic interactions between the monomers and establishes an equilibrium between monomeric and trimeric PS1. (C) Cooling to 20 °C (solid lipid phase). PS1 monomers and trimers are surrounded by lipid molecules ("trapped equilibrium"). (D) Lipids of extracted PS1 complexes are replaced by the detergent β-DM. Due to the preseparation of monomeric PS1 in the thylakoid membrane, the isolation of intact PS1 monomers is possible; additionally, preexisting PS1 trimers are isolated.

Structural Implications of PS1 Monomers versus Trimers: Protein Part. Our results indicate that under physiological "low-salt" conditions the equilibrium is very much in favor of the PS1 trimer with a quite small amount of monomer being extracted. Omitting the salt step indicated that even the (high) salt treatment caused no detectable loss of subunits or pigments. Mass spectrometry analysis in combination with SDS−PAGE and immunoblot analysis showed the complete set of subunits both for the two monomer preparations and for the trimer preparation, in agreement with the data from the 3D X-ray structure of the trimer (*1*). The identical mass spectra of monomers (+ST and −ST) confirm the efficiency of the presented method and indicate that the complete assembly of PS1 should occur before the oligomerization process, in agreement with results obtained for *Synechocystis* (*62*). It was reported that the PsaL subunit is essential (together with PsaM and PsaI) for the trimerization process (*1*, *46*, *63*−*65*), and it was also shown that PsaL is easily lost during the isolation procedure (*3*, *45*, *50*). In contrast, both −ST and +ST monomers of our preparation retained their PsaL subunit, confirming the extremely mild isolation conditions used in our approach.

Additionally, this report could show for the first time the complete analysis of modifications for all subunits, yielding essentially no difference between monomers and trimers. Interestingly, the same types of modifications have been shown for PS2 subunits from *T. elongatus*, and these have been correlated with the orientation of the subunits within the complex (*66*, *67*). According to this analysis, N-termini of PS2 subunits facing the lumen seem to stay formylated, whereas N-termini facing the cytoplasmic side are modified by cleavage of the first amino acid, probably because they are accessible for processing enzymes. Similar results have been gained for the Cyt b_6f complex (*66*). However, this model does not fit completely for the PS1 subunits: PsaK and PsaM are processed, although their N-termini are exposed to the lumen (*1*), and PsaJ still keeps the initial formyl modification while its N-terminus faces the cytoplasm. This suggests a different mechanism for the assembly of PS1, especially concerning its subunits PsaK, PsaM, and PsaJ, in comparison with PS2 or the Cyt b_6f complex.

Finally, the combination of salt treatment and "routine" detergent extraction allows the isolation of at least 10 times more monomeric PS1 than the "extreme mild treatment" and for this reason was established as a routine preparation procedure for monomers with upscaling capacity.

Structural and Functional Implications of PS1 Monomers versus Trimers: Reaction Center and Antenna Chls. Spectroscopic analysis such as the 5 K absorption spectra (Figure 2) or the determination of the pigment content (Table 2) suggests that PS1 monomers closely resemble PS1 trimers. The Chl/P700 ratio, reflecting the Chl antenna size per PS1, is higher than that reported for other PS1 preparations from *T. elongatus* and for the 3D crystal structure of the trimer from the same organism. While the first HPLC-purified monomeric PS1 displayed, like the trimer, 85 ± 5 Chls/P700 [determination of P700 by light-induced absorption change (*38*, *50*)], this value could not be improved by a different preparation procedure, yielding 85 or 65 Chls/P700 upon extraction by β-DM or sulfobetaine 12, respectively (*45*); this is possibly due to the harsh treatment during the preparation process. In contrast, our monomeric complexes showed ∼108 ± 7 Chls/P700 (trimer, 112 ± 8 Chls/P700), indicating that there is no loss of antenna pigments during the preparation, although these numbers might be slightly too large due to the used extinction difference coefficient (see Results). The Chl/Car ratio is within the error margins the same for PS1 monomers and trimers, resulting in ∼22 Cars per PS1 which is in agreement with the X-ray structure (*1*). These results indicate that the antenna size and organization do not change during the oligomerization process and confirm the conclusion that the improved isolation method gave nativelike PS1 monomers.

There is one interesting exception. At 5 K, the absorption spectrum of trimeric PS1 shows a shoulder around 720 nm that is

less pronounced in the monomers. According to analysis by Gaussian deconvolution, the PS1 monomers contain approximately two fewer LWCs than the trimers (see Table 2), which is also confirmed by the 5 nm blue shift in the 77 K fluorescence emission peak of the monomers (−ST and +ST) compared to the trimers (see Figure 4A). This effect can be used as a "quality control" for isolated PS1 monomers. There is also agreement with previous results obtained with *A. platensis*, where characteristic 77 K main fluorescence peaks of monomeric and trimeric PS1 (730 and 760 nm, respectively) confirmed the successful in vitro oligomerization of isolated monomeric PS1 from *A. platensis* into trimer (*31*).

PS1 monomer preparations reported previously also contained a smaller amount of LWCs (*24*) which has been attributed mainly to the absence of the L-subunit leading to the loss of LWCs located in the trimerization domain (*27*). Since the nativelike PS1 monomers of this report, too, exhibit a decreased red-most absorption band, two explanations seem feasible. (a) It is quite possible that trimerization causes conformational changes of assembled monomers which lead to a stronger coupling of two (or more) Chl molecules; this may induce formation of a Chl aggregate within each monomer, resulting in an increased red-shifted absorption. (b) Alternatively, strong interaction between peripheral Chls of different monomers within the trimer might lead to a red-shifted low-energy exciton band. Two such Chls can be identified, for instance, from the X-ray structure of *T. elongatus* trimers: Chl 11601 coordinated by subunit M of one monomer and Chl 11801 coordinated by a phospholipid of the other (Chl numbering according to Protein Data Bank entry 1JB0) approach by the trimerization to an edge-to-edge distance of ∼5 Å. Especially the M subunit-coordinated Chl is not well connected to the energy transfer network within the monomer, but apparently better connected to Chls of the adjacent monomer. We may assume that both Chls play an important role in the transfer of energy among the monomers integrated within the trimer (for a more detailed discussion, see refs *15* and *68*). If we attribute the additional LWCs in the PS1 trimer to these two Chls, the distance of this red trap would be ∼45 Å with respect to P700. It should be noted that Car 7 is closest to the proposed M1−P1 dimer with an edge-to-edge distance of ∼5 Å to P1 and to M1 of the adjacent monomer.

Most recently, a time-resolved analysis revealed two kinetically different "red" Chl pools in monomeric and trimeric PS1 complexes from *T. elongatus* (*69*) isolated according to the method outlined here. Because of the mild preparation conditions, the origin of the red compartments in the monomer could be compared with that of the trimer. These results indicated that both types of LWCs originate from the same forms of pigments in either the monomeric or oligomeric state. It is not clear why the two additional LWCs observed in trimers could not be revealed in these data.

The number of Chls that are disconnected from the Chl antenna network is another indicator for the quality of a preparation. Such Chls lose their ability to transfer energy to other Chls which results in a fluorescence emission at ∼670−680 nm. The fact that both PS1 monomers and trimers at 77 K showed no emission at this wavelength confirms the absence of such Chls in our preparations (see Figure 4A). At RT, fluorescence emission spectra of the various PS1 preparations show a shoulder at 688−695 nm in both monomers, which is significantly smaller in trimers (Figure 4B). This might be partly explained by the larger number of red Chls leading to a stronger localization of the excitation on the red states. In addition, this might be an effect of the bound detergent concentration. The surface area which is exposed to the detergent β-DM most probably is larger for monomers than for trimers; this results in a tension force that affects peripherally located Chls and causes both a small shift and a disconnection from the antenna network. A further increase in the detergent concentration or the use of more aggressive detergents would result in a loss of these Chls due to incorporation into detergent micelles. This would explain the lower Chl/PS1 ratio observed in earlier PS1 preparations.

Spectral properties of the reaction center can be monitored by time-resolved absorption difference spectroscopy. Absorbance difference spectra reflect the changes in absorption upon light-induced formation of transient functional states (charge-separated states or ^{3}P700) within the reaction center. Due to the difference, only pigments with altered electronic state and pigments coupled to them contribute to the spectra. In this work, we measured the flash-induced absorption difference spectra of PS1 monomers and trimers attributed to the formation of $P700^+F_{A/B}^-$ at RT (Figure 3A) and 5 K (Figure 3B). As even the high-resolution spectra at 5 K were almost identical for monomers and trimers, this indicates identical spectral properties and an identical arrangement of the reaction center pigments. In addition, the identical midpoint potential for P700 in monomers and trimers strongly suggests that the surroundings of P700 and the redox properties of the components involved in electron transfer do not change upon oligomerization (Table 2).

The light-induced electron transport activity (DPIP → MV) is also the same for PS1 trimers and monomers using high-white light illumination. The rate of ∼1350 μmol of O_2 (mg of Chl)$^{-1}$ h^{-1} corresponds to the transport of 55 electrons per PS1 per second, with the rate-limiting step being most likely the donation of an electron to $P700^+$ by DPIP. Using red and far-red illumination, the electron transport activity is higher for trimers than for monomers (see Table 2). This higher efficiency of trimers in the far-red region can be related to their higher LWC content which might contribute by uphill-energy transfer to P700, especially under low-light conditions (*19*, *35*).

Physiological Implications of PS1 Dynamics. The comparison of nativelike PS1 monomers, produced by various procedures, with PS1 trimers revealed that monomers most probably preexist in thylakoid membranes in equilibirium with trimers. As indicated by our extraction under extremely mild conditions, this equilibrium under "normal", i.e., stress-free, conditions is very much in favor of trimeric PS1, leaving less than 10% of all PS1 for the monomer. A similar ratio has also been found for membranes of the mesophilic cyanobacterium *Synechococcus* PCC 7002 (*65*).

The physiological significance of this monomer−trimer equilibrium may be many-fold. (1) Especially in the case of thermophilic organisms such as *T. elongatus*, the trimer may be dominant because of its higher stability based on hydrophobic effects that increase with temperature; this was recently shown by FTIR nvestigations (Kopczak, Dzafic, Mäntele, and Rögner, unpublished observations). (2) Besides better thermostability, the PS1 trimers may also yield a higher photostability due to the higher content of red-most chlorophylls which help in the dissipation of excess absorbed energy (*36*). (3) Stress conditions such as Fe limitation (*70*) have been reported to induce monomerization. Combined with this, the dynamic adaptation to changing light conditions by rearrangement of phycobilisome contact with the photosystems (known as state transitions) may

be induced by reversible monomerization/trimerization, which has been suggested (*61*, *65*). (4) Especially the structural and functional integrity of the monomer strongly indicates a role as an intermediate complex in PS1 biogenesis (*62*) prior to assembly of the trimer. This is in agreement with the case of photosystem 2 from the same organism, where a fully competent monomeric PS2 could be shown to precede the dimeric complex (*52*), but different from the case of the cytochrome b_6f complex, which requires the formation of a dimer for gaining activity (Gomolla and Rögner, unpublished observations). While the dynamics of monomeric PS2 complexes as "intermediates" in biogenesis and repair could be shown due to the high turnover rate of their D1 subunit (*52*), such processes are considerably delayed in the case of PS1 with reported lifetimes of several days (*71*). For this reason, we had to increase the very low steady state concentration of monomeric PS1 "artificially" by changing the ionic strength of the medium to gain sufficient material for comparative characterization with the trimer. Such a change in equilibrium may occur under physiological conditions by light and/or other stress conditions which still must be shown.

However, prerequisite for all these dynamic adaptations is an appropriate fluidity of the membrane which has been shown in this report for *T. elongatus*. The combination of all reported processes indicates a considerable potential for the dynamics of PS1 in the thylakoid membrane and may be the basis for its longevity and stress tolerance. Moreover, the comparison with PS2 shows that the monomer−oligomer equilibrium in the membrane is a universal mechanism for the regulation of the activity and stability of the photosynthetic apparatus.

Conclusions. (1) Monomeric PS1 is fully competent for all major reactions of trimeric PS1 and can be isolated as an intact complex with identical antenna size, subunit composition (including posttranslational modifications), and photochemical activity. (2) The dynamic equilibrium between the PS1 monomer and trimer in the thylakoid membrane is under nonstress conditions by far on the side of the trimers and is governed by the phase transition temperature of the surrounding lipids. (3) The structural equilibrium between monomer and trimer is reflected by a "functional" equilibrium with the trimer showing two additional long-wavelength chlorophylls.

ACKNOWLEDGMENT

We thank Claudia König and Regina Oworah-Nkruma for excellent technical assistance.

SUPPORTING INFORMATION AVAILABLE

Details of the biochemical isolation procedure, including quantification of the monomer/trimer ratio by HPLC elution profiles and sucrose density gradient centrifugation. This material is available free of charge via the Internet at http://pubs.acs.org.

REFERENCES

1. Jordan, P., Fromme, P., Witt, H. T., Klukas, O., Saenger, W., and Krauss, N. (2001) Three-dimensional structure of cyanobacterial photosystem I at 2.5 Å resolution. *Nature 411*, 909–917.
2. Fromme, P., Jordan, P., and Krauss, N. (2001) Structure of photosystem I. *Biochim. Biophys. Acta 1507*, 5–31.
3. Fromme, P., Melkozernov, A., Jordan, P., and Krauss, N. (2003) Structure and function of photosystem I: Interaction with its soluble electron carriers and external antenna systems. *FEBS Lett. 555*, 40–44.
4. Xu, Q., Yu, L., Chitnis, V. P., and Chitnis, P. R. (1994) Function and organization of photosystem I in a cyanobacterial mutant strain that lacks PsaF and PsaJ subunits. *J. Biol. Chem. 269*, 3205–3211.
5. Chitnis, P. R. (2001) Photosystem I: Function and Physiology. *Annu. Rev. Plant Physiol. Plant Mol. Biol. 52*, 593–626.
6. Nelson, N., and Yocum, C. F. (2006) Structure and function of photosystems I and II. *Annu. Rev. Plant Biol. 57*, 521–565.
7. Amunts, A., Drory, O., and Nelson, N. (2007) The structure of a plant photosystem I supercomplex at 3.4 Å resolution. *Nature 447*, 58–63.
8. Boekema, E. J., Dekker, J. P., van Heel, M. G., Rögner, M., Saenger, W., Witt, I., and Witt, H. T. (1987) Evidence for a trimeric organization of the photosystem I complex from the thermophilic cyanobacterium *Synechococcus* sp.. *FEBS Lett. 217*, 283.
9. Shubin, V. V., Tsuprun, V. L., Bezsmertnaya, I. N., and Karapetyan, N. V. (1993) Trimeric forms of the photosystem I reaction center complex pre-exist in the membranes of the cyanobacterium *Spirulina platensis*. *FEBS Lett. 334*, 79–82.
10. Fromme, P. (2003) Crystallization of Photosystem I. In Methods and Results in Crystallization of Membrane Proteins (Iwata, S., Ed.) pp 145−173, International University Line, La Jolla, CA.
11. Fromme, P., Schlodder, E., and Jansson, S. (2003) Structure and Function of the Antenna System in Photsystem I. In Light-Harvesting Antennas in Photosynthesis (Green, B. R., and Parson, W. W., Eds.) pp 253−279, Kluwer Academic Publishers, Dordrecht, The Netherlands.
12. Boekema, E. J., Jensen, P. E., Schlodder, E., van Breemen, J. F., van Roon, H., Scheller, H. V., and Dekker, J. P. (2001) Green plant photosystem I binds light-harvesting complex I on one side of the complex. *Biochemistry 40*, 1029–1036.
13. Ben-Shem, A., Frolow, F., and Nelson, N. (2003) Crystal structure of plant photosystem I. *Nature 426*, 630–635.
14. Klimmek, F., Ganeteg, U., Ihalainen, J. A., van Roon, H., Jensen, P. E., Scheller, H. V., Dekker, J. P., and Jansson, S. (2005) Structure of the higher plant light harvesting complex I: *In vivo* characterization and structural interdependence of the Lhca proteins. *Biochemistry 44*, 3065–3073.
15. Sener, M. K., Park, S., Lu, D., Damjanovic, A., Ritz, T., Fromme, P., and Schulten, K. (2004) Excitation migration in trimeric cyanobacterial photosystem I. *J. Chem. Phys. 120*, 11183–11195.
16. Sener, M. K., Jolley, C., Ben-Shem, A., Fromme, P., Nelson, N., Croce, R., and Schulten, K. (2005) Comparison of the light-harvesting networks of plant and cyanobacterial photosystem I. *Biophys. J. 89*, 1630–1642.
17. Shubin, V. V., Bezsmertnaya, I. N., and Karapetyan, N. V. (1992) Isolation from *Spirulina* membranes of two photosystem I-type complexes, one of which contains chlorophyll responsible for the 77 K fluorescence band at 760 nm. *FEBS Lett. 309*, 340–342.
18. van der Lee, J., Bald, D., Kwa, S., Grondelle, R., Rögner, M., and Dekker, J. (1993) Steady-state polarized light spectroscopy of isolated Photosystem I complexes. *Photosynth. Res. 35*, 311–321.
19. Karapetyan, N. V., Holzwarth, A. R., and Rögner, M. (1999) The photosystem I trimer of cyanobacteria: Molecular organization, excitation dynamics and physiological significance. *FEBS Lett. 460*, 395–400.
20. Gobets, B., and van Grondelle, R. (2001) Energy transfer and trapping in photosystem I. *Biochim. Biophys. Acta 1507*, 80–99.
21. Melkozernov, A. N., Lin, S., Blankenship, R. E., and Valkunas, L. (2001) Spectral inhomogeneity of photosystem I and its influence on excitation equilibration and trapping in the cyanobacterium *Synechocystis* sp. PCC6803 at 77 K. *Biophys. J. 81*, 1144–1154.
22. Karapetyan, N. V., Schlodder, E., van Grondelle, R., and Dekker, J. P. (2006) The long wavelength chlorophylls of photosystem I. In Photosystem I. The Light-Driven Plastocyanin: Ferredoxin Oxidoreductase (Golbeck, J. H., Ed.) pp 177−192, Springer, Dordrecht, The Netherlands.
23. Schlodder, E., Shubin, V. V., El-Mohsnawy, E., Rögner, M., and Karapetyan, N. V. (2007) Steady-state and transient polarized absorption spectroscopy of photosystem I complexes from the cyanobacteria *Arthrospira platensis* and *Thermosynechococcus elongatus*. *Biochim. Biophys. Acta 1767*, 732–741.
24. Palsson, L.-O., Dekker, J. P., Schlodder, E., Monshouwer, R., and Grondelle, R. (1996) Polarized site-selective fluorescence spectroscopy of the long-wavelength emitting chlorophylls in isolated Photosystem I particles of *Synechococcus elongatus*. *Photosynth. Res. 48*, 239–246.
25. Palsson, L. O., Flemming, C., Gobets, B., van Grondelle, R., Dekker, J. P., and Schlodder, E. (1998) Energy transfer and charge separation in photosystem I: P700 oxidation upon selective excitation of the long-wavelength antenna chlorophylls of *Synechococcus elongatus*. *Biophys. J. 74*, 2611–2622.

26. Byrdin, M., Rimke, I., Schlodder, E., Stehlik, D., and Roelofs, T. A. (2000) Decay Kinetics and Quantum Yields of Fluorescence in Photosystem I from *Synechococcus elongatus* with P700 in the Reduced and Oxidized State: Are the Kinetics of Excited State Decay Trap-Limited or Transfer-Limited? *Biophys. J. 79*, 992.
27. Byrdin, M., Jordan, P., Krauss, N., Fromme, P., Stehlik, D., and Schlodder, E. (2002) Light harvesting in photosystem I: Modeling based on the 2.5 Å structure of photosystem I from *Synechococcus elongatus*. *Biophys. J. 83*, 433–457.
28. Hayes, J. M., Matsuzaki, S., Ratsep, M., and Small, G. J. (2000) Red Chlorophyll a Antenna States of Photosystem I of the Cyanobacterium *Synechocystis* sp. PCC 6803. *J. Phys. Chem. B 104*, 5625–5633.
29. Rätsep, M., Johnson, T. W., Chitnis, P. R., and Small, G. J. (2000) The Red-Absorbing Chlorophyll a Antenna States of Photosystem I: A Hole-Burning Study of *Synechocystis* sp. PCC 6803 and Its Mutants. *J. Phys. Chem. B 104*, 836–847.
30. Karapetyan, N. V., Dorra, D., Schweitzer, G., Bezsmertnaya, I. N., and Holzwarth, A. R. (1997) Fluorescence spectroscopy of the long-wave chlorophylls in trimeric and monomeric photosystem I core complexes from the cyanobacterium *Spirulina platensis*. *Biochemistry 36*, 13830–13837.
31. Kruip, J., Karapetyan, N. V., Terekhova, I. V., and Rögner, M. (1999) In vitro oligomerization of a membrane protein complex. Liposome-based reconstitution of trimeric photosystem I from isolated monomers. *J. Biol. Chem. 274*, 18181–18188.
32. Schlodder, E., Cetin, M., Byrdin, M., Terekhova, I. V., and Karapetyan, N. V. (2005) $P700^+$- and $^3P700$-induced quenching of the fluorescence at 760 nm in trimeric Photosystem I complexes from the cyanobacterium *Arthrospira platensis*. *Biochim. Biophys. Acta 1706*, 53–67.
33. Karapetyan, N. V. (2008) Protective dissipation of excess absorbed energy by photosynthetic apparatus of cyanobacteria: Role of antenna terminal emitters. *Photosynth. Res. 97*, 195–204.
34. Trissl, H. W. (1993) Long-wavelength absorbing antenna pigments and heterogeneous absorption bands concentrate excitons and increase absorption cross section. *Photosynth. Res. 35*, 247–263.
35. Shubin, V. V., Bezsmertnaya, I. N., and Karapetyan, N. V. (1995) Efficient energy transfer from the long-wavelength antenna chlorophylls to P700 in photosystem I complexes from *Spirulina platensis*. *J. Photochem. Photobiol., B 30*, 153–160.
36. Karapetyan, N., Shubin, V. V., and Strasser, R. (1999) Energy exchange between the chlorophyll antennae of monomeric subunits within the Photosystem I trimeric complex of the cyanobacterium *Spirulina*. *Photosynth. Res. 61*, 291–301.
37. Almog, O., Shoham, G., Michaeli, D., and Nechushtai, R. (1991) Monomeric and trimeric forms of photosystem I reaction center of *Mastigocladus laminosus*: Crystallization and preliminary characterization. *Proc. Natl. Acad. Sci. U.S.A. 88*, 5312–5316.
38. Rögner, M., Mühlenhoff, U., Boekema, E. J., and Witt, H. T. (1990) Mono-, di- and trimeric PS I reaction center complexes isolated from the thermophilic cyanobacterium *Synechococcus* sp.: Size, shape and activity. *Biochim. Biophys. Acta 1015*, 415–424.
39. Schafheutle, M. E., Setlikova, E., Timmins, P. A., Johner, H., Gutgesell, P., Setlik, I., and Welte, W. (1990) Molecular weight determination of an active photosystem I preparation from a thermophilic cyanobacterium, *Synechococcus elongatus*. *Biochemistry 29*, 1216–1225.
40. Hladík, J., Pancoska, P., and Sofrová, D. (1982) The influence of carotenoids on the conformation of chlorophyll-protein complexes isolated from the cyanobacterium *Plectonema boryanum*. Absorption and circular dichroism study. *Biochim. Biophys. Acta 681*, 263–272.
41. Fromme, P., and Witt, H. T. (1998) Improved isolation and crystallization of photosystem I for structural analysis. *Biochim. Biophys. Acta 1365*, 175–184.
42. Mühlenhoff, U., and Chauvat, F. (1996) Gene transfer and manipulation in the thermophilic cyanobacterium *Synechococcus elongatus*. *Mol. Gen. Genet. 252*, 93–100.
43. Chitnis, V. P., Xu, Q., Yu, L., Golbeck, J. H., Nakamoto, H., Xie, D. L., and Chitnis, P. R. (1993) Targeted inactivation of the gene psaL encoding a subunit of photosystem I of the cyanobacterium *Synechocystis* sp. PCC 6803. *J. Biol. Chem. 268*, 11678–11684.
44. Domonkos, I., Malec, P., Sallai, A., Kovacs, L., Itoh, K., Shen, G., Ughy, B., Bogos, B., Sakurai, I., Kis, M., Strzalka, K., Wada, H., Itoh, S., Farkas, T., and Gombos, Z. (2004) Phosphatidylglycerol is essential for oligomerization of photosystem I reaction center. *Plant Physiol. 134*, 1471–1478.
45. Jekow, P., Fromme, P., Witt, H. T., and Saenger, W. (1995) Photosystem I from *Synechococcus elongatus*: Preparation and crystallization of monomers with varying subunit compositions. *Biochim. Biophys. Acta 1229*, 115–120.
46. Grotjohann, I., and Fromme, P. (2005) Structure of cyanobacterial photosystem I. *Photosynth. Res. 85*, 51–72.
47. Rakhimberdieva, M. G., Boichenko, V. A., Karapetyan, N. V., and Stadnichuk, I. N. (2001) Interaction of phycobilisomes with photosystem II dimers and photosystem I monomers and trimers in the cyanobacterium *Spirulina platensis*. *Biochemistry 40*, 15780–15788.
48. Kruip, J., Bald, D., Boekema, E. J., and Rögner, M. (1994) Evidence for the existence of trimeric and monomeric Photosystem I complexes in thylakoid membranes from cyanobacteria. *Photosynth. Res. 40*, 279–286.
49. Lax, J. E., Arteni, A. A., Boekema, E. J., Pistorius, E. K., Michel, K. P., and Rögner, M. (2007) Structural response of Photosystem 2 to iron deficiency: Characterization of a new photosystem 2-IdiA complex from the cyanobacterium *Thermosynechococcus elongatus* BP-1. *Biochim. Biophys. Acta 1767*, 528–534.
50. Rögner, M., Nixon, P. J., and Diner, B. A. (1990) Purification and characterization of photosystem I and photosystem II core complexes from wild-type and phycocyanin-deficient strains of the cyanobacterium *Synechocystis* PCC 6803. *J. Biol. Chem. 265*, 6189–6196.
51. Wenk, S. O., and Kruip, J. (2000) Novel, rapid purification of the membrane protein photosystem I by high-performance liquid chromatography on porous materials. *J. Chromatogr., B 737*, 131–142.
52. Nowaczyk, M. M., Hebeler, R., Schlodder, E., Meyer, H. E., Warscheid, B., and Rögner, M. (2006) Psb27, a cyanobacterial lipoprotein, is involved in the repair cycle of photosystem II. *Plant Cell 18*, 3121–3131.
53. Lichtenthaler, H. K. (1987) Chlorophylls and carotenoids: Pigments of photosynthetic biomembranes. In Methods in Enzymology (Packer, L., and Douce, R., Eds.) pp 350−382, Academic Press, London.
54. Witt, H., Bordignon, E., Carbonera, D., Dekker, J. P., Karapetyan, N., Teutloff, C., Webber, A., Lubitz, W., and Schlodder, E. (2003) Species-specific differences of the spectroscopic properties of P700: Analysis of the influence of non-conserved amino acid residues by site-directed mutagenesis of photosystem I from *Chlamydomonas reinhardtii*. *J. Biol. Chem. 278*, 46760–46771.
55. Flemming, C. (1996) Ph.D. Thesis, Technische Universität Berlin, Berlin.
56. Porra, R. J., Thompson, W. A., and Kriedemann, P. E. (1989) Determination of accurate extinction coefficients and simultaneous equations for assaying chlorophylls a and b extracted with four different solvents: Verification of the concentration of chlorophyll standards by atomic absorption spectroscopy. *Biochim. Biophys. Acta 975*, 384–394.
57. Liaaen-Jensen, S., and Jensen, A. (1971) Quantitative determination of carotenoids in photosynthetic tissues. In Methods in Enzymology (Colowick, S. P., and Kaplan, N. O., Eds.) pp 586−602, Academic Press, London.
58. Chitnis, P. R., Purvis, D., and Nelson, N. (1991) Molecular cloning and targeted mutagenesis of the gene psaF encoding subunit III of photosystem I from the cyanobacterium *Synechocystis* sp. PCC 6803. *J. Biol. Chem. 266*, 20146–20151.
59. Kruip, J., Boekema, E. J., Bald, D., Boonstra, A. F., and Rögner, M. (1993) Isolation and structural characterization of monomeric and trimeric photosystem I complexes ($P700 \cdot F_A/F_B$ and $P700 \cdot F_X$) from the cyanobacterium *Synechocystis* PCC 6803*. *J. Biol. Chem. 268*, 23353–23360.
60. Kis, M., Zsiros, O., Farkas, T., Wada, H., Nagy, F., and Gombos, Z. (1998) Light-induced expression of fatty acid desaturase genes. *Proc. Natl. Acad. Sci. U.S.A. 95*, 4209–4214.
61. Bald, D., Kruip, J., and Rögner, M. (1996) Supramolecular architecture of cyanobacterial thylakoid membranes: How is the phycobilisome connected with the photosystems? *Photosynth. Res. 49*, 103.
62. Dühring, U., Ossenbühl, F., and Wilde, A. (2007) Late assembly steps and dynamics of the cyanobacterial photosystem I. *J. Biol. Chem. 282*, 10915–10921.
63. Chitnis, V. P., and Chitnis, P. R. (1993) PsaL subunit is required for the formation of photosystem I trimers in the cyanobacterium *Synechocystis* sp. PCC 6803. *FEBS Lett. 336*, 330–334.
64. Xu, Q., Hoppe, D., Chitnis, V. P., Odom, W. R., Guikema, J. A., and Chitnis, P. R. (1995) Mutational analysis of photosystem I polypeptides in the cyanobacterium *Synechocystis* sp. PCC 6803. Targeted inactivation of psaI reveals the function of psaI in the structural organization of psaL. *J. Biol. Chem. 270*, 16243–16250.
65. Schluchter, W. M., Shen, G., Zhao, J., and Bryant, D. A. (1996) Characterization of psaI and psaL mutants of *Synechococcus* sp.

strain PCC 7002: A new model for state transitions in cyanobacteria. *Photochem. Photobiol. 64*, 53–66.
66. Nowaczyk, M. M. (2005) Ph.D. Thesis, Ruhr-Universiät Bochum, Bochum, Germany.
67. Guskov, A., Kern, J., Gabdulkhakov, A., Broser, M., Zouni, A., and Saenger, W. (2009) Cyanobacterial photosystem II at 2.9 Å resolution and the role of quinones, lipids, channels and chloride. *Nat. Struct. Mol. Biol. 16*, 334–342.
68. Fromme, P., and Grotjohann, I. (2006) Structural Analysis of Cyanobacterial Photosystem I. In Photosystem I. The Light-Driven Plastocyanin:Ferredoxin Oxidoreductase (Golbeck, J. H., Ed.) pp 47−69, Springer, Dordrecht, The Netherlands.
69. Slavov, C., El-Mohsnawy, E., Rögner, M., and Holzwarth, A. R. (2009) Trapping kinetics in isolated cyanobacterial PS I complexes. *Chem. Phys. 357*, 163–170.
70. Ivanov, A. G., Krol, M., Sveshnikov, D., Selstam, E., Sandstrom, S., Koochek, M., Park, Y. I., Vasilev, S., Bruce, D., Oquist, G., and Huner, N. P. (2006) Iron deficiency in cyanobacteria causes monomerization of photosystem I trimers and reduces the capacity for state transitions and the effective absorption cross section of photosystem I in vivo. *Plant Physiol. 141*, 1436–1445.
71. Henderson, J. N., Zhang, J., Evans, B. W., and Redding, K. (2003) Disassembly and degradation of photosystem I in an *in vitro* system are multievent, metal-dependent processes. *J. Biol. Chem. 278*, 39978–39986.